AD-A248 345

Finite Difference Modelling of Seismic
Wave Propagation at the Seafloor

R. A. Stephen
RASCON Associates

DTIC
SELECTE
S D
D

92-06684

92 T 18 097

REPORT DOCUMENTATION PAGE

Public reporting burden for this collection of information is estimated to average 1 hour per response, including the time for reviewing instructions, searching existing data sources, gathering and maintaining the data needed, and completing and reviewing the collection of information. Send comments regarding this burden or any other aspect of this collection of information, including suggestions for reducing this burden, to Washington Headquarters Services, Directorate for Information Operations and Reports, 1215 Jefferson Davis Highway, Suite 1204, Arlington, VA 22202-4302, and to the Office of Management and Budget, Paperwork Reduction Project (0704-0188), Washington, DC 20503.

1. Agency Use Only *(Leave blank)*.	2. Report Date. 1991	3. Report Type and Dates Covered. Final - Contractor Report

4. Title and Subtitle.
Finite Difference Modelling of Seismic Wave Propagtion

5. Funding Numbers.

Contract	N00014-88-M-6610
Program Element No.	0602435N
Project No.	03501
Task No.	JOZ
Accession No.	DN258112
Work Unit No.	13628G

6. Author(s).
R. A. Stephen*

7. Performing Organization Name(s) and Address(es).
*RAFCON, Associates
W. Falmouth, MA 02574

8. Performing Organization Report Number.

9. Sponsoring/Monitoring Agency Name(s) and Address(es).
Naval Oceanographic and Atmospheric Research Laboratory
Ocean Science Directorate
Stennis Space Center, MS 39529-5004

10. Sponsoring/Monitoring Agency Report Number.
CR 026:91

11. Supplementary Notes.

12a. Distribution/Availability Statement.
Approved for public release; distribution is unlimited.

12b. Distribution Code.

13. Abstract *(Maximum 200 words)*.

The objectives of this study were i) to implement the WHOI finite difference code on the CONVEX computer at NORDA and ii) to run a suite of models on the effects of lateral heterogeneity on the primary response from the seafloor.

Finite difference solutions to the elastic wave equation accurately predict the response of impulsive and continuous wave sources in media with arbitrary vertical and horizontal variation, with fluid-solid interfaces and with shear propagation in the solid. All possible wave types are included (reflections, refractions, diffractions, Stoneley and pseudo-Rayleigh waves, evanescent waves and head waves). The primary disadvantage of the method is that it is very computation intensive and it is generally limited to problems with dimensions of only a few tens of wavelengths. This can be partially alleviated by using powerful computers such as the CONVEX at NORDA.

14. Subject Terms.
Seismic, Acoustic, Modelling

15. Number of Pages. 26

16. Price Code.

17. Security Classification of Report. Unclassified	18. Security Classification of This Page. Unclassified	19. Security Classification of Abstract. Unclassified	20. Limitation of Abstract. SAR

FINITE DIFFERENCE MODELLING OF SEISMIC WAVE PROPAGATION AT THE SEAFLOOR

Final Technical Report for NORDA Contract #N00014-88-M-6610

R.A. Stephen
RASCON Associates
P.O. Box 567
W. Falmouth, MA 02574

1. INTRODUCTION

The objectives of this study were i) to implement the WHOI finite difference code on the CONVEX computer at NORDA and ii) to run a suite of models on the effects of lateral heterogeneity on the primary response from the seafloor.

Finite difference solutions to the elastic wave equation accurately predict the response of impulsive and continuous wave sources in media with arbitrary vertical and horizontal variation, with fluid-solid interfaces and with shear propagation in the solid. All possible wave types are included (reflections, refractions, diffractions, Stoneley and pseudo-Rayleigh waves, evanescent waves and head waves). The primary disadvantage of the method is that it is very computation intensive and it is generally limited to problems with dimensions of only a few tens of wavelengths. This can be partially alleviated by using powerful computers such as the CONVEX at NORDA.

This proposal addressed the following categories in NORDA-BAA-88-2:

1) Acoustic ASW oceanography

   b) ultra low and very low frequency propagation

   i) acoustic transients

   j) low frequency arctic acoustics

   o) acoustic field interactions (scattering)

2) Non-acoustic oceanographic measurements

   i) bathymetry

   j) geophysics

5) Computer Modelling

   e) geoacoustic extensions to environmental acoustic prediction systems.

The latter item, 5)e), is the particular focus of the proposal.

2. THE FINITE DIFFERENCE METHOD

The finite difference technique (Stephen, 1988) is a powerful method for studying the complete sea bottom interaction of the acoustic field in the ocean. Because the computational effort is quite large the method is generally restricted to low frequencies (5-25 Hz) but in many cases it is at these frequencies where bottom interaction becomes important. Because the method is based in the time domain it is particularly well suited to pulse or transient problems. The technique also has considerable promise for studying scattering from ice in arctic acoustics. The code lends itself well to extending acoustic forward modelling schemes to include geoacoustic bottom properties.

Stephen (1988) has reviewed the finite difference method as applied to bottom interaction problems. A number of applications including focusing of deterministic structure (Stephen, 1984; Dougherty and Stephen, 1987; Stephen, 1988) and scattering from random seafloor (Dougherty and Stephen, 1988) have been presented. Also the code has been calibrated by comparison with other methods such as the reflectivity method (Stephen, 1983) and by participating in the benchmark sessions at the Acoustical Society of America meetings (Stephen, submitted). We have sufficient experience with the code that we are confident that it will be useful in studying bottom interaction problems in range dependent environments including shear wave effects in the bottom. NORDA should be interested in the results.

3. IMPLEMENTATION OF THE FINITE DIFFERENCE CODE AT NORDA

The objective here was to install the WHOI finite difference code on the CONVEX and to run test models at 10Hz out to 10 km for a full ocean depth of 5.5 km. Deep models like this had not been run before so we made a number of modifications before we could run this model successfully. The models are described in section 4. Here we review the modifications that were made and describe where the files are on the CONVEX.

A finite difference model is run in three steps: i) a preprocessor which sets up the necessary arrays for a given calculation; ii) a program to compute the elastic parameters and density in a transition zone near the seafloor; and iii) the actual finite difference calculations. Software for each stage including makefiles for compilation is located in /mnt/stephen/prep, /mnt/stephen/bny, /mnt/stephen/diff respectively on the CONVEX. A macro (or command file) for each model run is located in that model's subdirectory. For example, the macro for model BBNY1 is located in /obs3b/stephen/bbny1/bbny1.bch. Once the parameter file is defined a model can be run by submitting the .bch file to the batch queue. More details on the structure and implementation of the code can be found in Hunt et al (1983).

In /mnt/stephen/diff are all the versions of the finite difference code used in this study. SFINDIF.FOR is the main driving code for all cases. The changes occur in the subroutines SDUMTS* and SBIBTS*, which actually carry out the template calculations, and in the subroutines SFINSUB* and SBIBSUB* which carry out the absorbing boundary calculations.

We used two templates. Initially we used the Bhasavanija template (Stephen et al, 1985; Stephen, 1988) however this resulted in instabilities at the fluid/solid interface at large times. The second template is based on a formulation presented by Virieux (1986). This produces stable and accurate results for a wide range of models.

We used two absorbing boundary schemes. The first was based on a parabolic equation approximation right at the boundary and the second was based on the telegraph equation applied in a region near the boundary. The telegraph equation has terms which introduce attenuation into the grid.

The original WHOI finite difference code used SDUMTS5 and SFINSUB4. This used a Bhasavanija template with parabolic equation boundaries on the right and bottom sides. (The top side is a free surface and the left side is an axis of symmetry.) Although adequate for small, short runs this was unstable on the bottom edge for the large models.

The next try (SBIBTS5 and SBIBSUB4) used the telegraph equation on the bottom edge only. This was unstable on the right boundary.

The third case (SBIBTS6 and SBIBSUB4) used the telegraph equation on the bottom edge and the right hand edge. The grid boundaries were stable, but an instability occurred at the seafloor at large times. After all of the principle phases had passed through the seafloor, a phase appeared at the interface which looked like a Stoneley wave. However its amplitude grew unrealistically with time. We call this the 'Bibee' instability. We do not recommend using SDUMTS5, SBIBTS5, SBIBTS6, SFINSUB4 and SBIBSUB4 for large models. They are on the CONVEX, however, for completeness.

In order to avoid the 'Bibee' instability we went to a Virieux formulation with the telegraph equation on the bottom edge and parabolic equation on the right edge (SBIBTS7 and SBIBSUB7). This fixed the 'Bibee' instability but there were false reflections from the right side.

Finally we used the telegraph equation on the right and bottom sides (SBIBTS9 and SBIBSUB7). This works fine and the test models in the next section use this formulation.

We also modified the WHOI code to output run time information and maximum amplitude values to the log file (*.LG4) during execution. This facilitates testing and provides a record of the run time for each job.

While testing we used the snapshot display on the SUN developed at NORDA. However, time series are more physically significant. To aid in the reading and plotting of the time series files (*.TST) we wrote a program, askii.f, which reads the binary file (*.TST) and writes an askii file (*.ASK). It is possible in askii.f to subsample the receiver locations. Askii.f can be used as the basis for any code that needs to read a *.TST file, such as plotting code or a seismic processing code.

4. SUITE OF TEST MODELS

In order to confirm that the finite difference code on the CONVEX actually solved problems of interest to NORDA, we ran a suite of six test models:

i) a range independent layered model representative of the seafloor (BBNY1);

ii) a model like i) but with bottom roughness (BBNY2);

iii) a model like i) but with basement roughness (BBNY3);

iv) a model like i) but with both bottom and basement roughness (BBNY4);

v) a model like i) but with a discontinuous high velocity stringer in the sediment (BBNY5);

vi) a model like i) but with a different shear velocity profile in the sediments and basement (BBNY6).

Each model on the CONVEX has its own subdirectory (/obs3b/stephen/bbny*). The model is run by submitting bbny*.bch to the batch queue. This file must be modified to include the correct *.PAR file (change all occurences of BBNY* to the same correct name). The makefile in /mnt/stephen/bny must be modified to use the correct bibbny*.f file in /mnt/stephen/bny. These files are used to generate the elastic parameters and densities in the transition zone and are usually written for each model. The files created by bbny*.bch are:

BBNY*.LG1 - log output of preprocessor

BBNY*.LG2 - log output of bibbny*.f

BBNY*.LG4 - log output of the finite difference calculation including run time parameters

BBNY*.TST - binary file of time series at receiver locations

BBNY*.SNS - binary files of the snapshot values (the last four values before the period give the timestep value divided by 10)

All models use a pressure source function which is the third derivative of a Gaussian pulse with a peak frequency of 10 Hz. A discussion of this pulse is given in

Appendix E of Stephen et al (1985). BBNY1 was run for 15,000 time steps (15 sec.) and all other models were run for 7,500 timesteps (7.5 sec).

The layout of the first model is given in Figure 1 and the velocity-depth functions and density depth functions are given in Figure 2 and Table 1. The pressure time series for a line of receivers at 4.98 km depth in BBNY1 (Figure 3) show stable results out to 15 sec for the primary bottom interaction and the first water multiple. At large offsets (greater than 3 km) there are shear wave peg leg multiples in the sediments. A weak reflection from the absorbing boundary can be identified after 13 seconds on the short range traces.

Figure 4 shows just the primary bottom interaction for BBNY1. The large first arrival is the direct wave from the source. The waveform varies because of the Lloyd's mirror effect with the sea surface. A weak first arrival is observed at ranges beyond 7.0 km which is the head wave. About 1.0 second behind the direct wave at short range is the seafloor reflection and about 0.5 second behind this is the basement reflection. This is all that is observed at short range except for some weak intra-bed multiples. At larger ranges there is later energy corresponding to shear wave multiples in the sediment. These data could be processed further using conventional analysis techniques to bring out more details but this is beyond the scope of this study.

The second model (BBNY2) is the same as the first except the seafloor varies sinusoidally with an amplitude of 100 m and a wavelength of 2.0 km. The first hill is directly below the shot. The parameters at the seafloor remain constant (as for BBNY1) and they vary linearly down to their values just above basement. The time series in Figure 5 only vary slightly from BBNY1 because they are dominated by the direct wave. The effects of bottom roughness can be seen in the amplitude variations of the seafloor reflection and head wave. The shear wave multiples have lost their coherence.

The third model (BBNY3) has a flat seafloor but a sinusoidally varying basement with an amplitude of 50 m and a wavelength of 3.0 km. The first valley is directly under the shot. Again values on the interfaces are constant with linear gradients running vertically

Figure 1. The layout in two dimensions of the finite difference grid used in this study.

SOURCE AT 10 (0.08 KM)

FREE SURFACE AT 2 (0 KM)

AXIS OF SYMMETRY

HOMOGENEOUS WATER
VP1=1.5 KM/SEC, VS1=0.0 KM/SEC, RO1=1.06H/CC

TRANSITION REGION

HOMOGENEOUS SOLID
VP2=6.0 KM/SEC, VS2=3.56KM/SEC, RO2=2.59 GM/CC

ABSORBING REGION

ABSORBING REGION

1 (0KM)

540 (5.38KM)

700 (6.98KM)

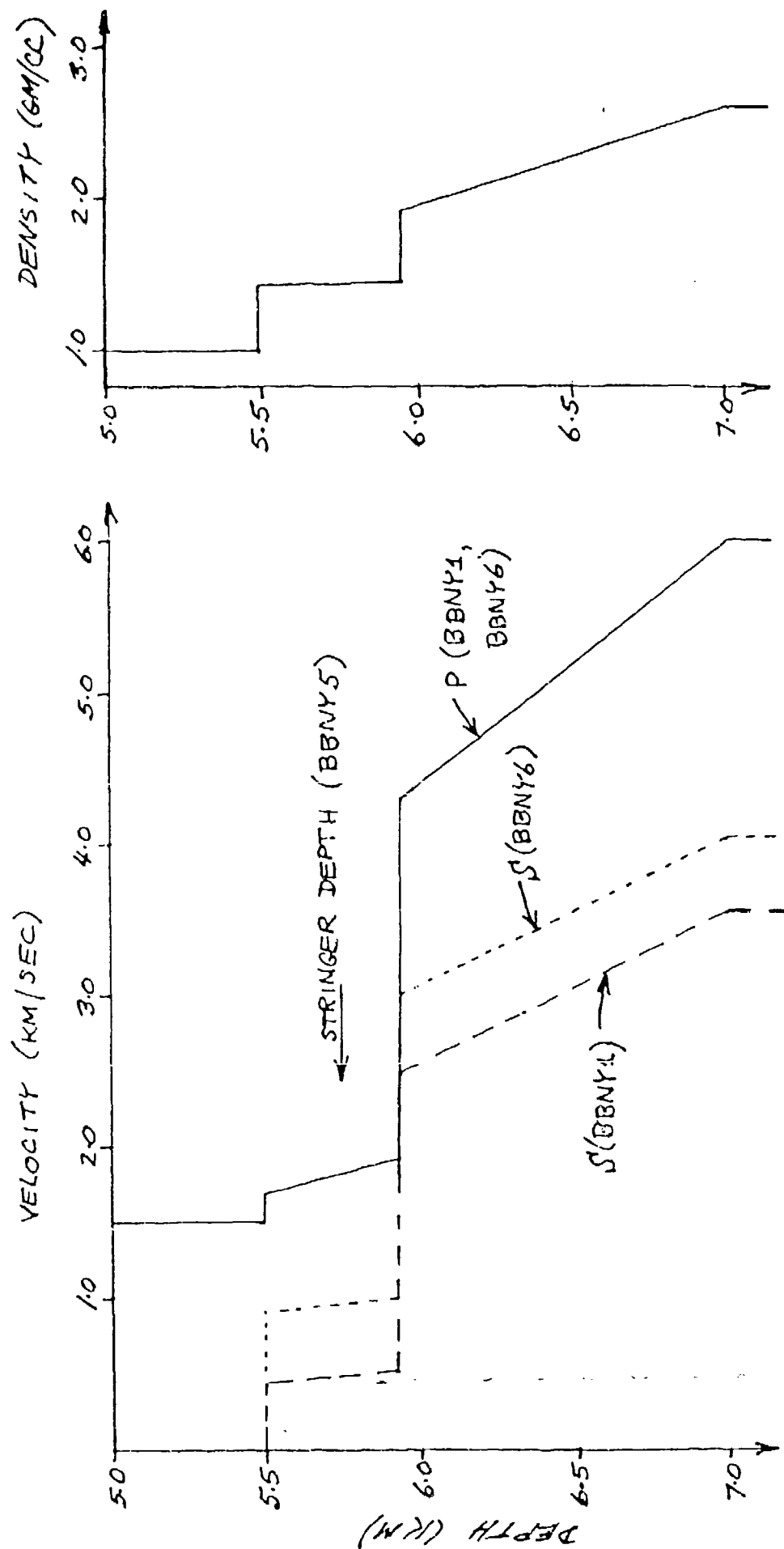710 (7.08KM)

800 (7.98KM)

910 (9.08KM)

1000 (9.92KM)

Figure 2. Summary of the velocity-depth and density-depth functions used for models BBNY1 and BBNY6.

TABLE 1. Velocity - Depth and Density - Depth Functions

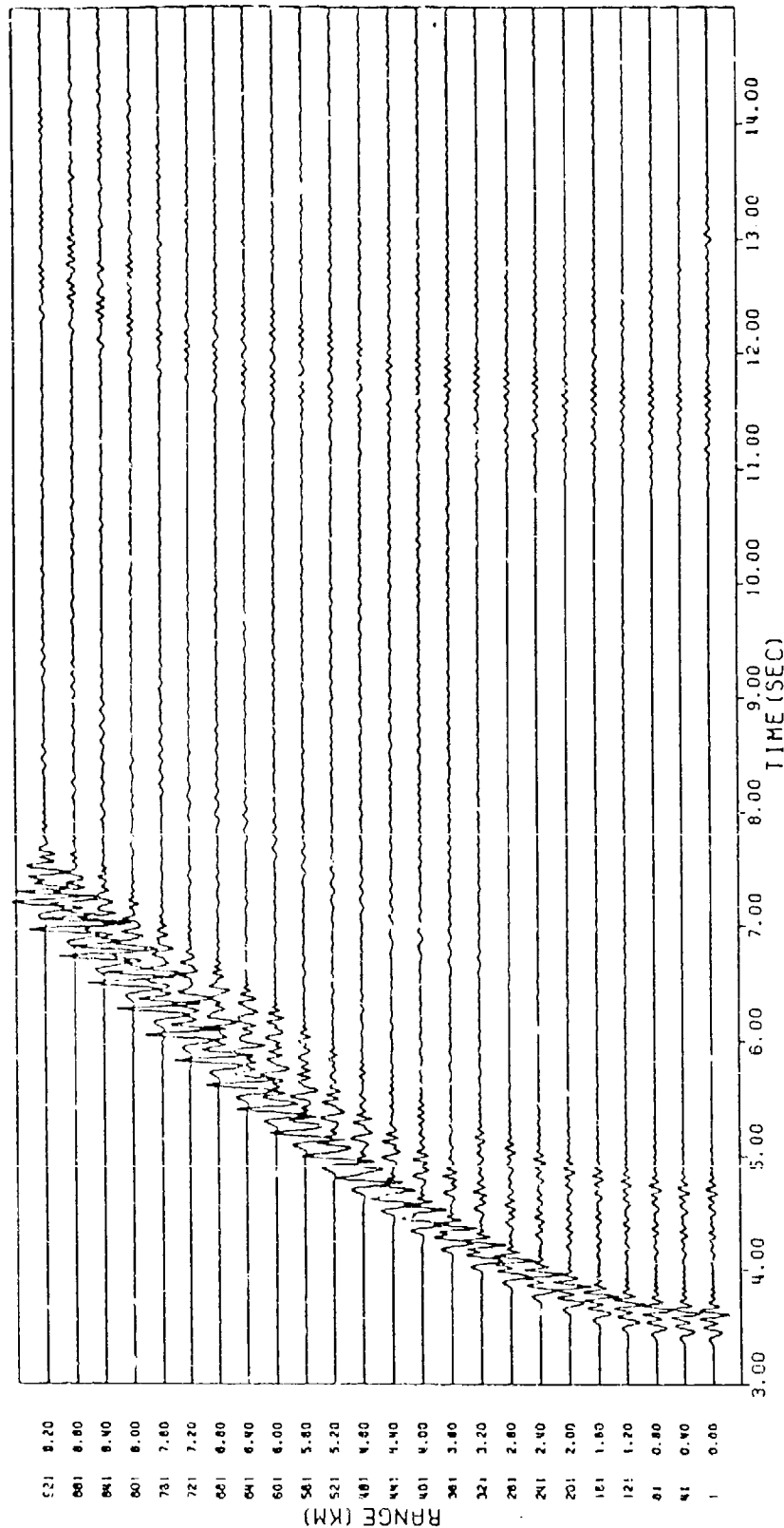| Depth (km)	P (BBNY1, BBNY6) (km/sec)	S (BBNY1) (km/sec)	POISSON'S RATIO (BBNY1)	S (BBNY6) (km/sec)	POISSON'S RATIO (BBNY6)	Density (gm/cc)
5.50 (above)	1.50	0.00	0.50	0.00	0.50	1.00
5.50 (below)	1.70	0.45	0.46	0.90	0.30	1.42
5.83 (above)	1.90	0.50	0.46	1.00	0.30	1.42
5.83 (below)	4.3	2.48	0.25	2.98	0.04	1.88
7.0 (above)	6.0	3.56	0.23	4.06	0.08	2.59
7.0 (below)	6.0	3.56	0.23	4.06	0.08	2.59

Figure 3a)

Figure 3. Time series results of the finite difference code for a line of pressure receivers at 4.98 km depth in model BRNY1. The time series extend to 15 seconds and show the primary and first water multiple. Figure 3a) has a gain of 1.0×10^{-7} and shows the direct wave unclipped. Figure 3b) has a gain of 1.25×10^{-6} and shows more of the low amplitude features such as the compressional head wave and the wide angle peg-leg multiples of shear waves in the sediments.
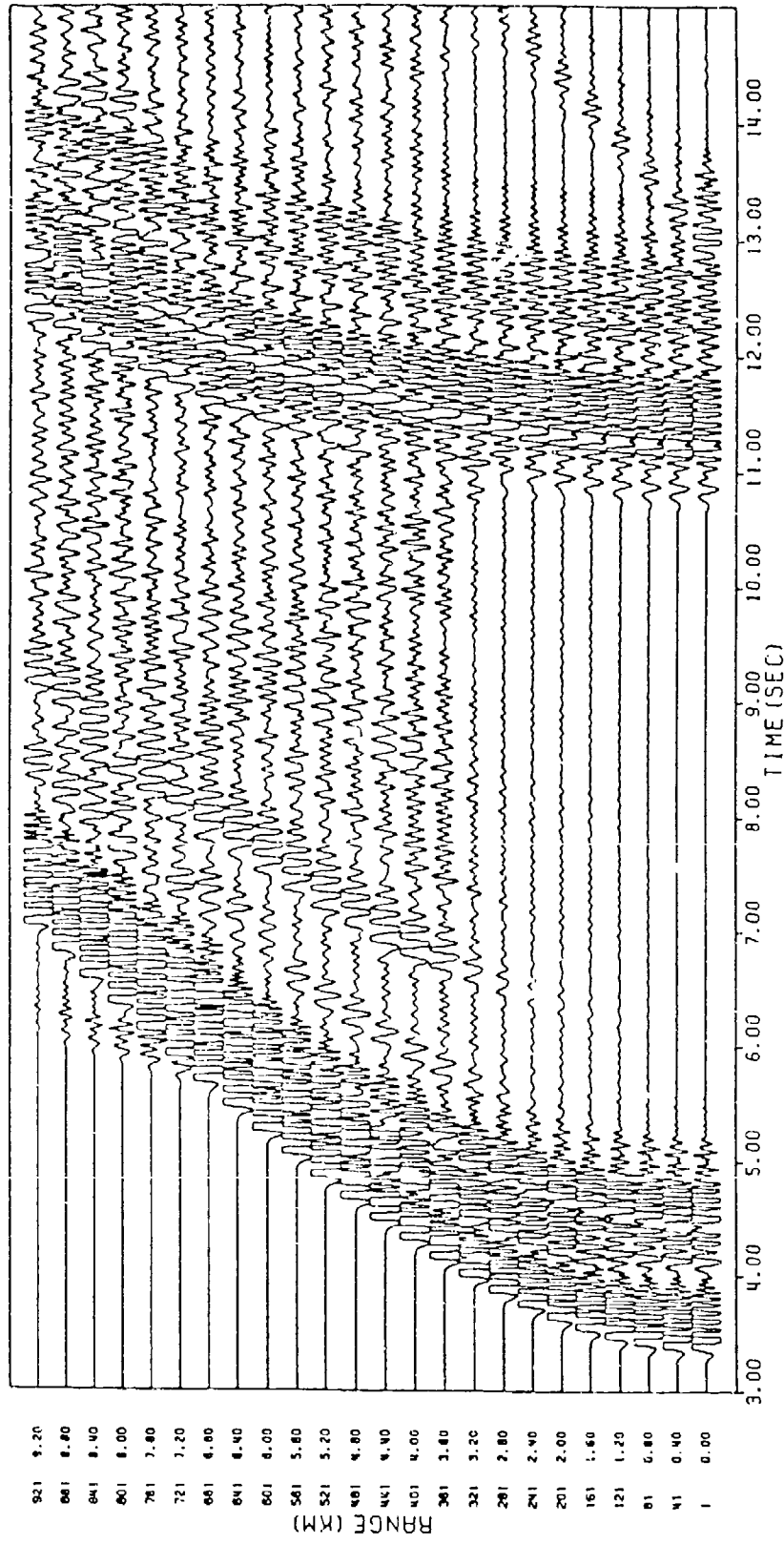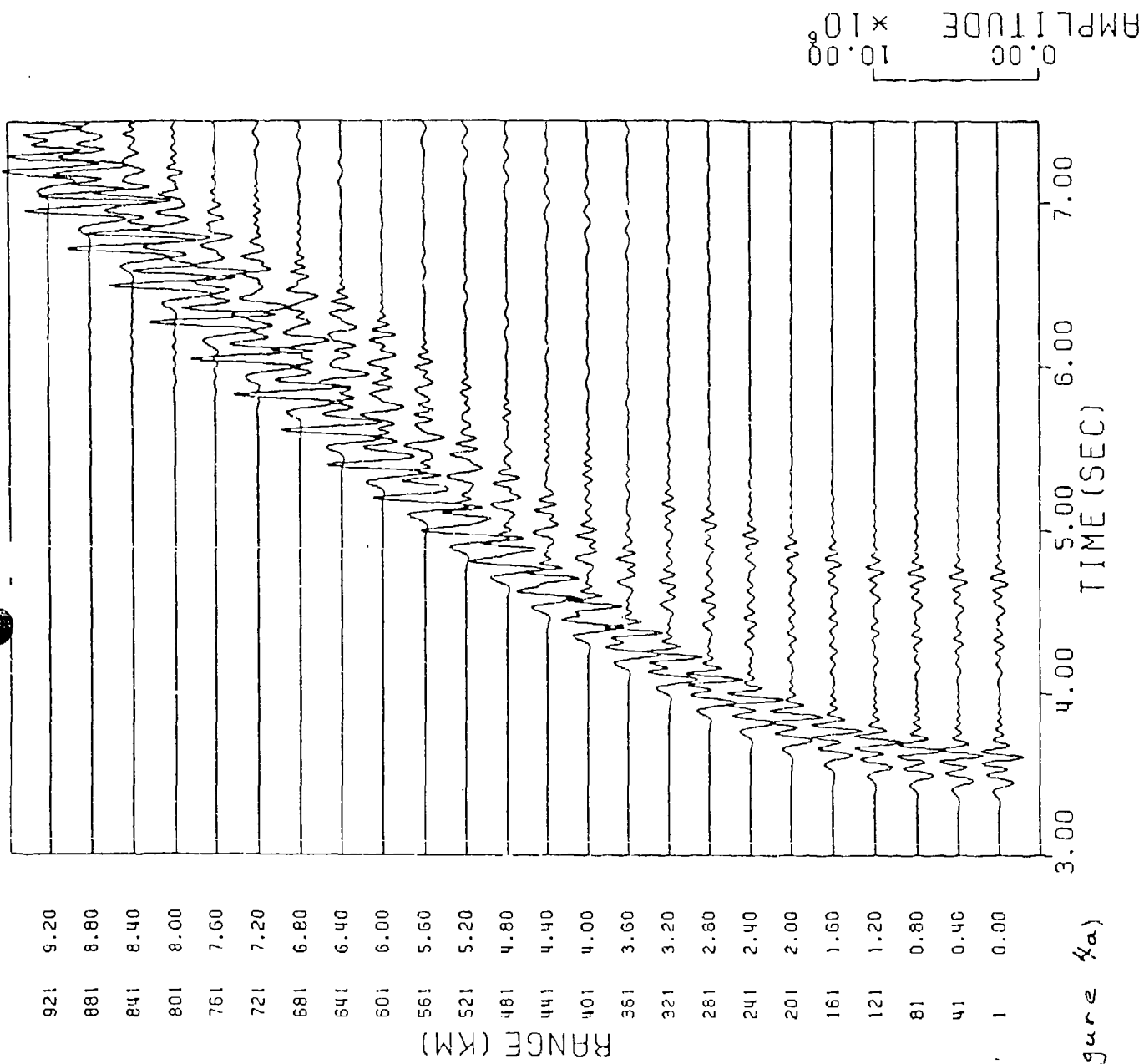
Figure 36)

Figure 4. This is a more detailed look of just the primary bottom interaction for model BBNY1. The gain levels for 4a) and 4b), and all subsequent figures are the same as for 3a) and 3b).
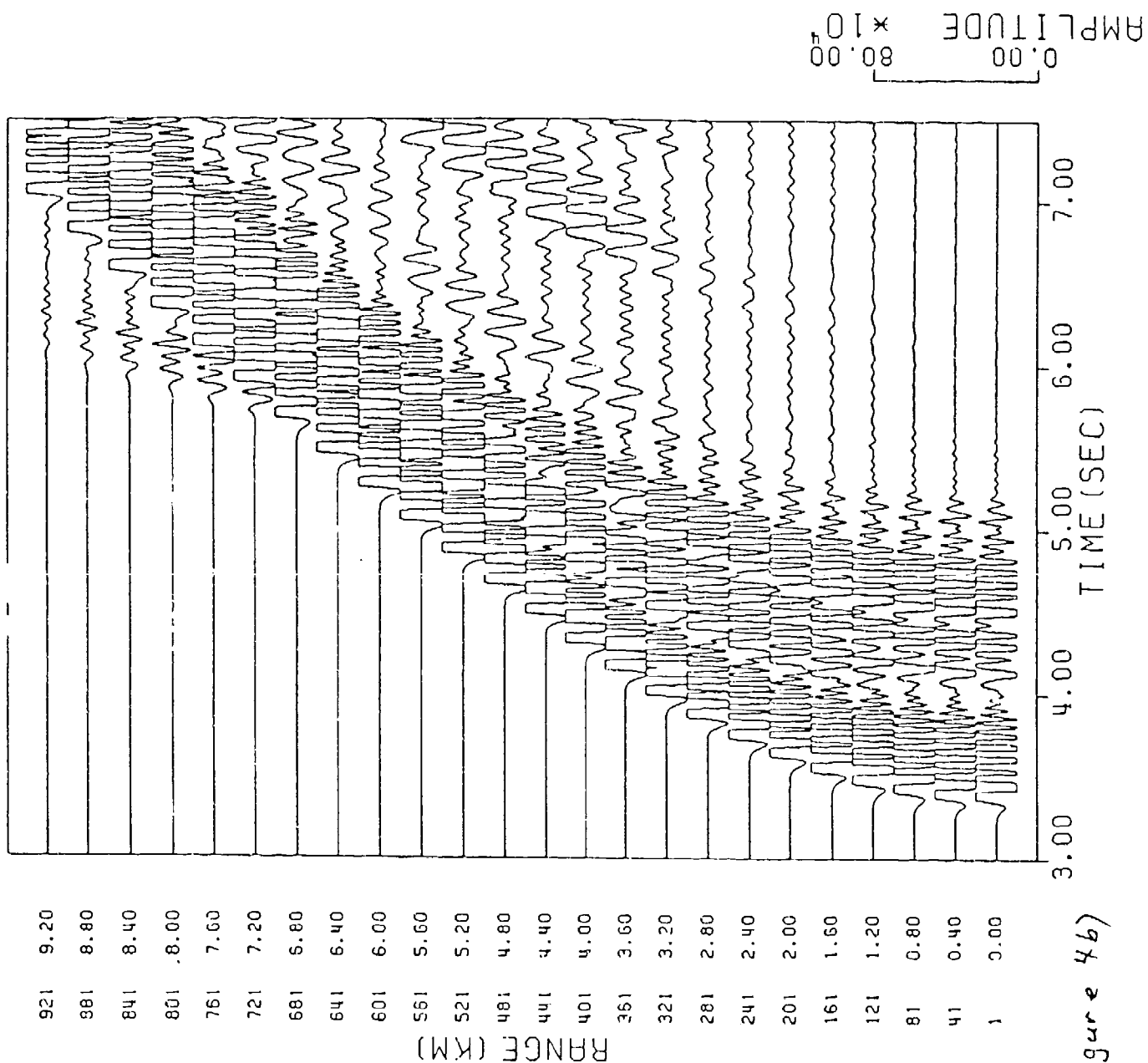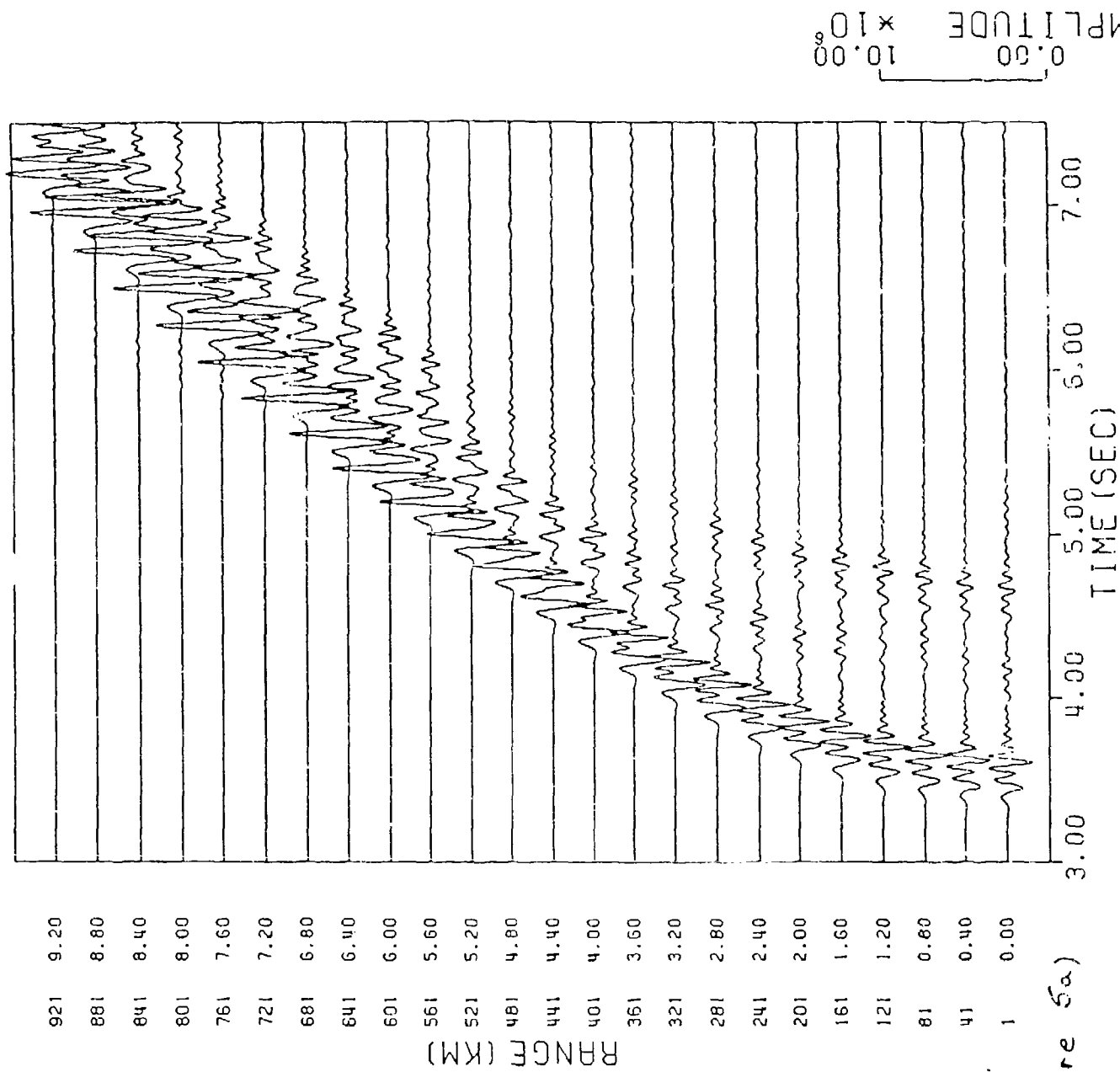
Figure 4b)

Figure 5. Time series results for a line of pressure receivers at 4.98 km depth in model BBNY2 with a sinusoidally undulating seafloor. The coherence of the peg-leg multiples is greatly reduced compared to the flat model (Figure 4).
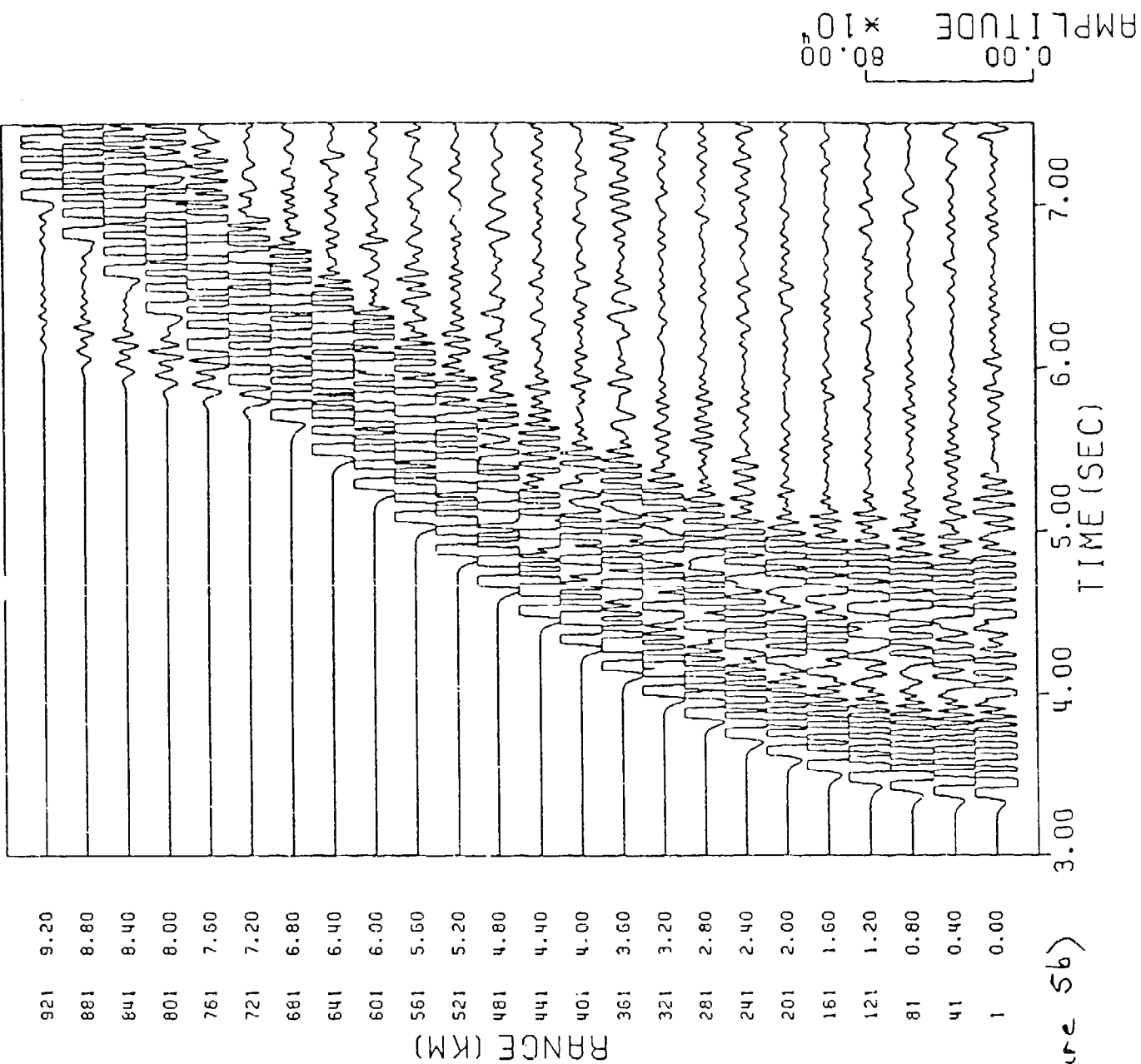
Figure 5a)

Figure 5b)

between the interfaces. Small changes in the amplitude and arrival time of the basement reflection occur (Figure 6).

The fourth model (BBNY4) combines the sinusoidal seafloor and basement of BBNY2 and BBNY3. The seafloor reflection is the same as for BBNY2 but the basement reflection varies from both BBNY3 and BBNY4 as expected (Figure 7). The snapshots for this relatively complex model should be particularly exciting.

The fifth model (BBNY5) is a flat model, as BBNY1, but it has a high velocity stringer V_p = 5.0 k/s, V_s = 2.88 k/s, and rho = 2.0 gm/cc) between 5.74 and 5.78 km depth and out to a range of 0.5 km (see Fig. 2). When this was originally run with a sharp contrast between the sediments and the stringer, the calculations were unstable. I do not understand this but it was fixed by averaging the parameters on the boundary values around the stringer. The time series on Figure 8 show a large reflection from this stringer masking basement at short range. At a range of 0.8 km the stringer is not influencing the trace. No diffractions are evident at this scale. The shear wave multiples at larger offsets are unaffected by the stringer.

The sixth model (BBNY6) demonstrates the effect of varying just the shear profile in a flat model such as BBNY1. Compressional velocity and density are unchanged but shear velocity is increased making both the sediments and basement more rigid (Figure 2). In BBNY1 Poisson's ratio in sediment and basement was 0.46 and about 0.25, respectively. In BBNY6 the corresponding Poisson's ratios are 0.30 and about 0.05 (Table 1). At short ranges the changes are insignificant but the coda have larger amplitude at large offsets due to wide angle shear wave reflections and multiples (Figure 9). A nice shear head wave is also evident just before the direct wave at ranges greater than 8.4 km.
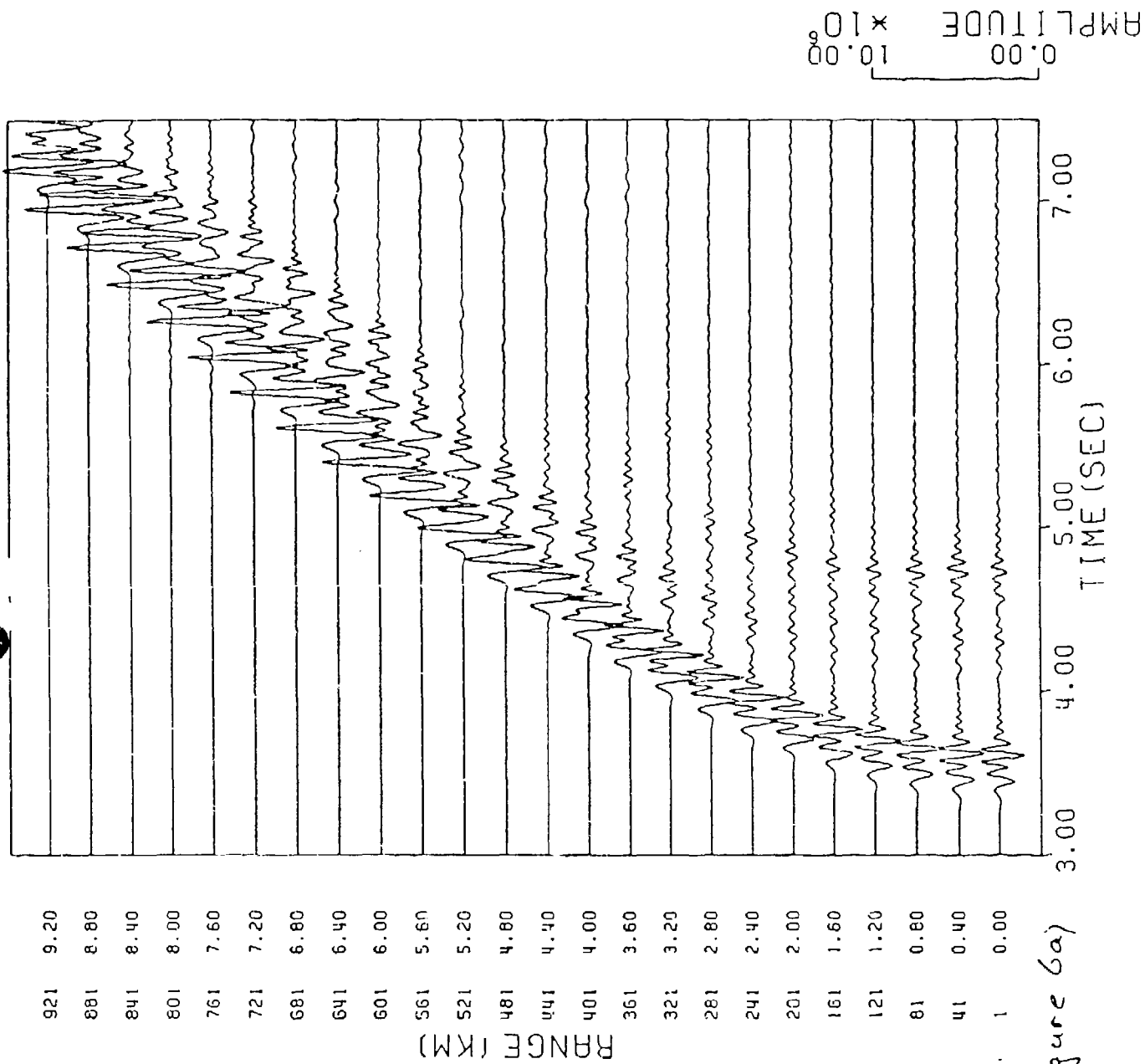
Figure 6. Time series results for a line of pressure receivers at 4.98 km depth in model BBNY3 with a flat seafloor but undulating basement.

AMPLITUDE ×10^4

0.00   8.00   0.00

TIME (SEC)

3.00   4.00   5.00   6.00   7.00

RANGE (KM)

921	9.20
881	8.80
841	8.40
801	8.00
761	7.60
721	7.20
681	6.80
641	6.40
601	6.00
561	5.60
521	5.20
481	4.80
441	4.40
401	4.00
361	3.60
321	3.20
281	2.80
241	2.40
201	2.00
161	1.60
121	1.20
81	0.80
41	0.40
1	0.00

Figure (6)

AMPLITUDE ×10⁶

0.00   10.00

RANGE (KM)

921   9.20
881   8.80
841   8.40
801   8.00
761   7.60
721   7.20
681   6.80
641   6.40
601   6.00
561   5.60
521   5.20
481   4.80
441   4.40
401   4.00
361   3.60
321   3.20
281   2.80
241   2.40
201   2.00
161   1.60
121   1.20
81   0.80
41   0.40
1   0.30

3.00   4.00   5.00   6.00   7.00

TIME (SEC)
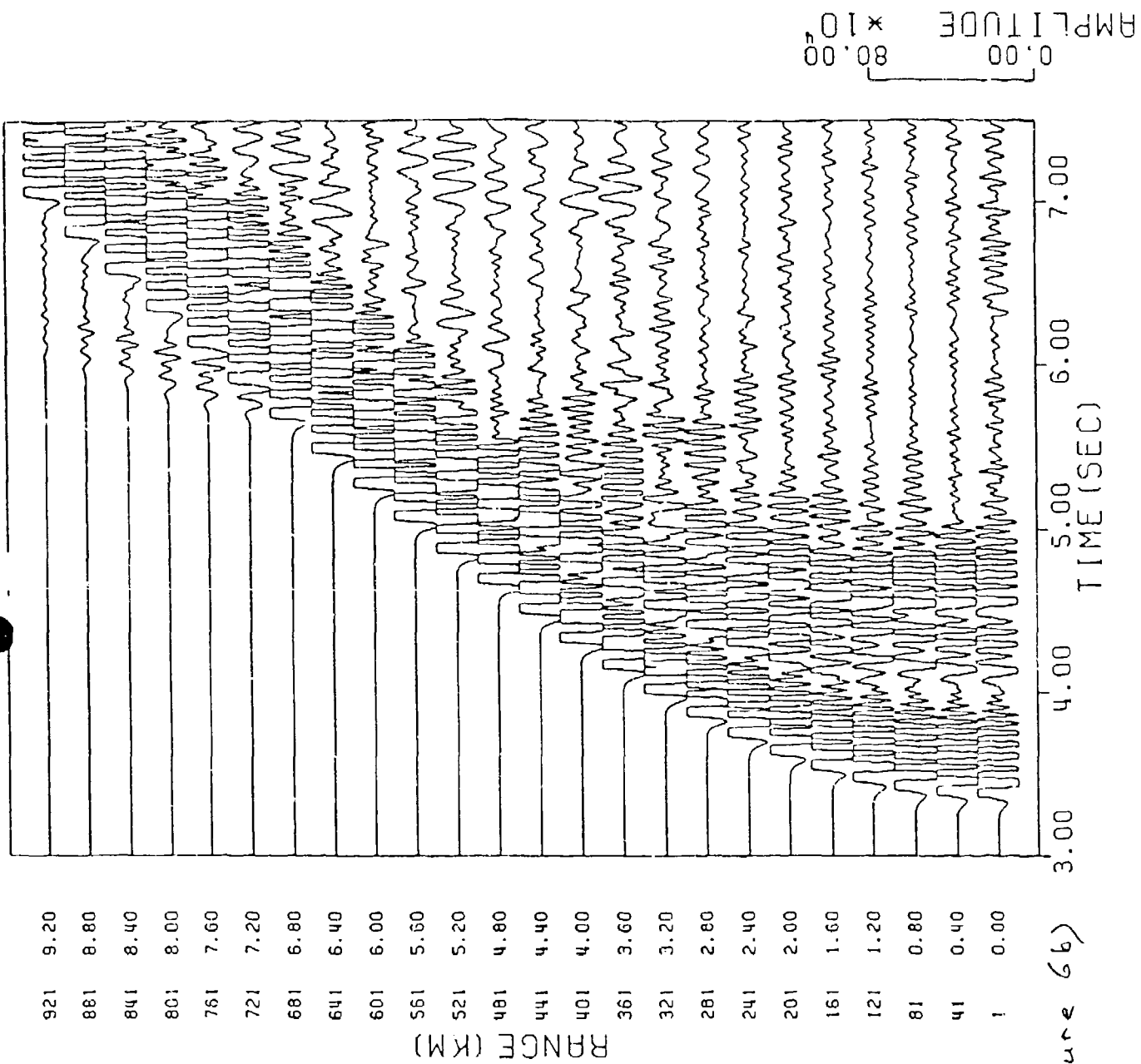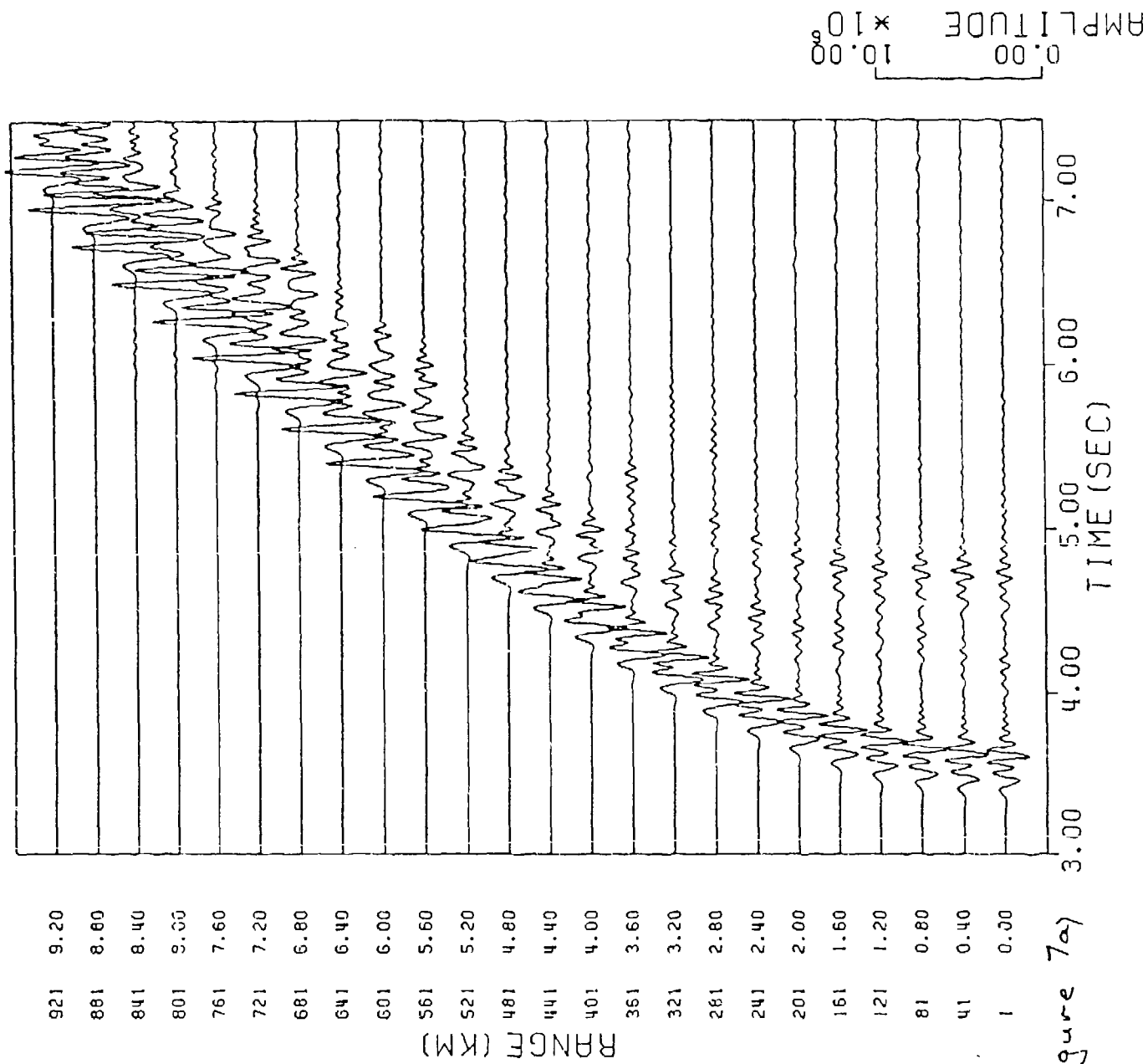
Figure 7a)

Figure 7. Time series results for a line of pressure receivers at 4.98 km depth in model BBNY4 with undulating surfaces for both the seafloor and basement.
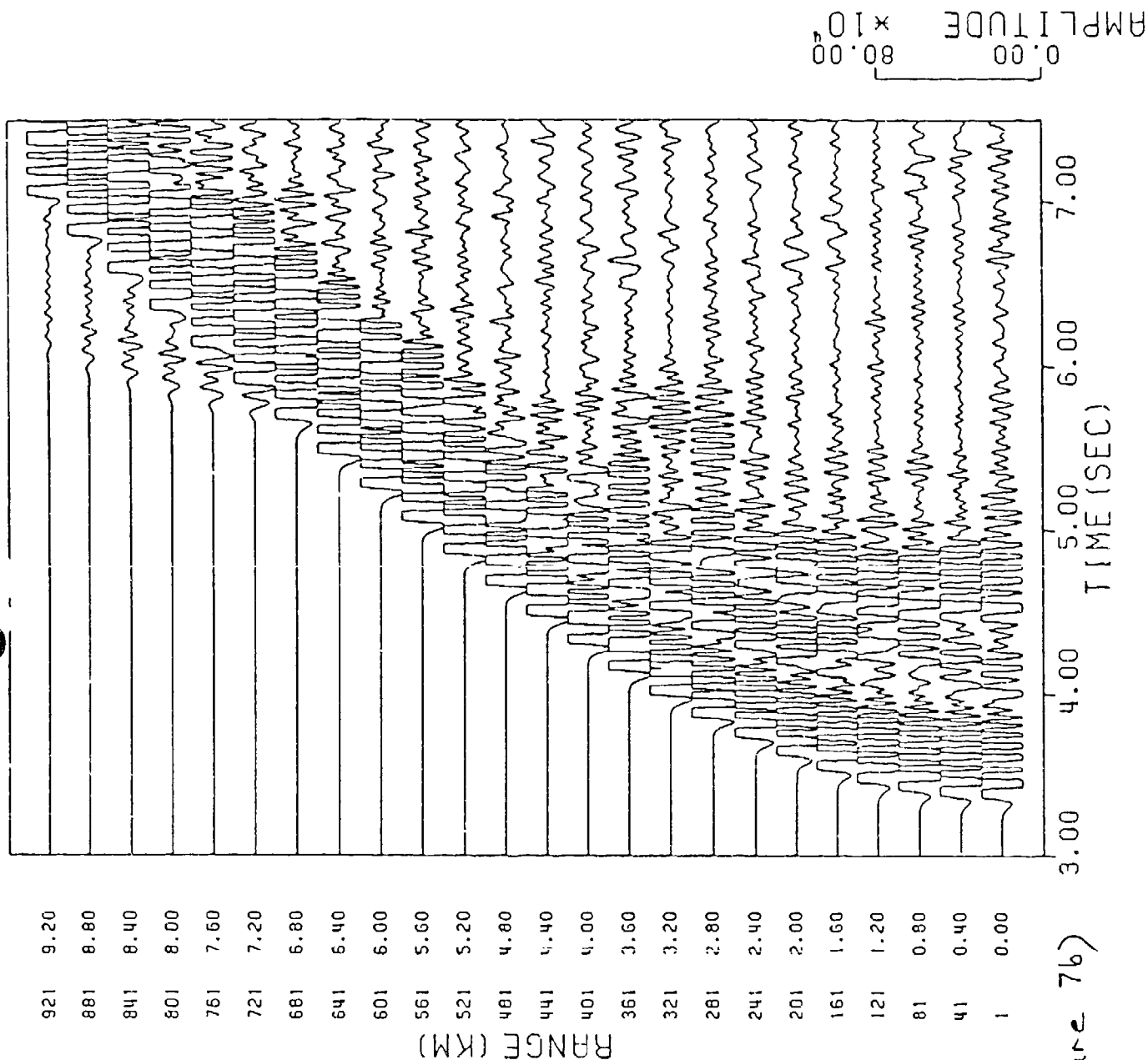
Figure 7b)

AMPLITUDE ×10⁶

10.00   0.00

RANGE (KM)

921	9.20
881	8.80
841	8.40
801	8.00
761	7.60
721	7.20
681	6.80
641	6.40
601	6.00
561	5.60
521	5.20
481	4.80
441	4.40
401	4.00
361	3.60
321	3.20
281	2.80
241	2.40
201	2.00
161	1.60
121	1.20
81	0.80
41	0.40
1	0.00

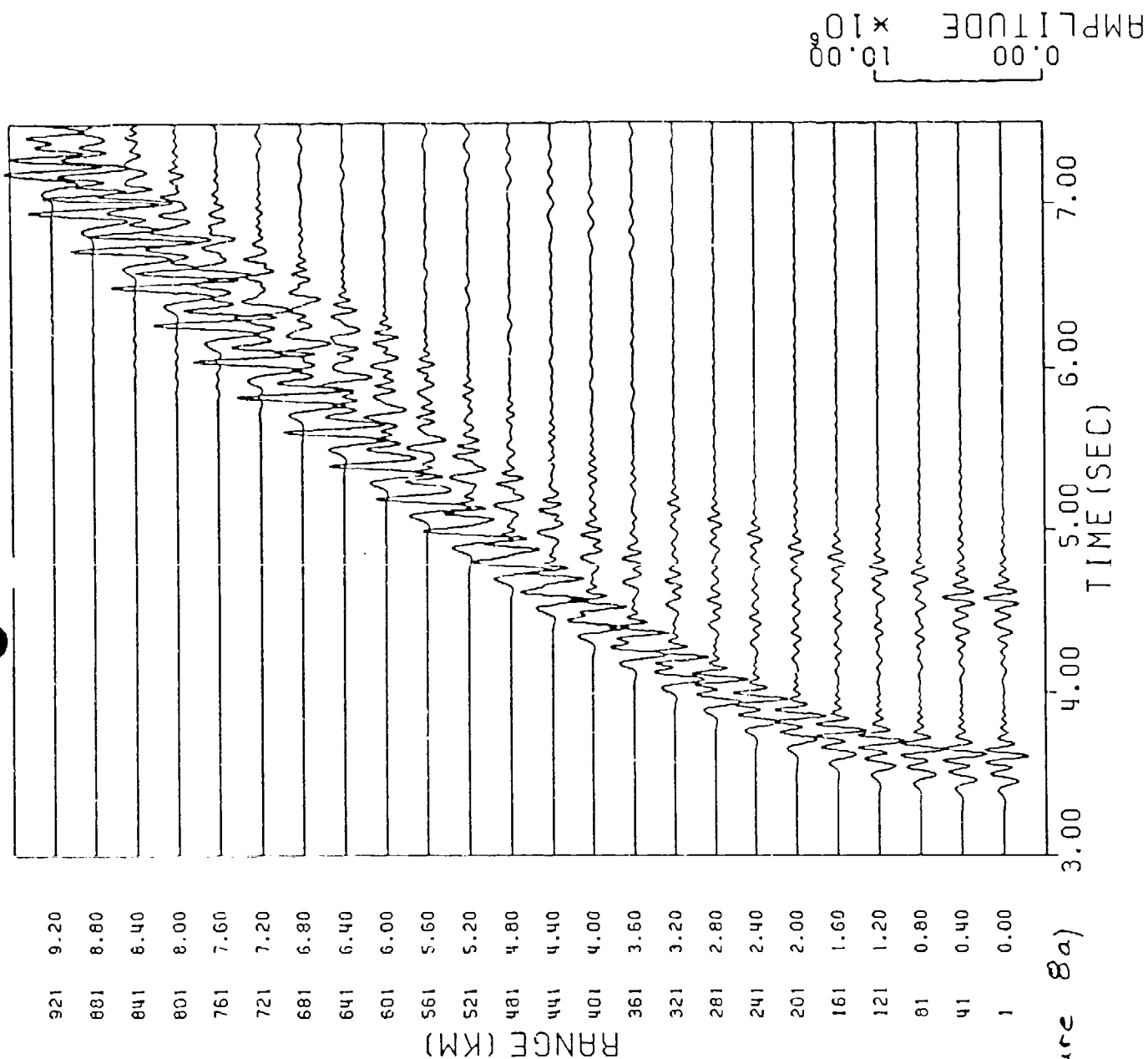3.00   4.00   5.00   6.00   7.00

TIME (SEC)

Figure 8a)

Figure 8. Time series results for a line of pressure receivers at 4.98 km depth in model BBNY5.
This is a flat model with a high velocity stringer just above basement. Reflections from the stringer
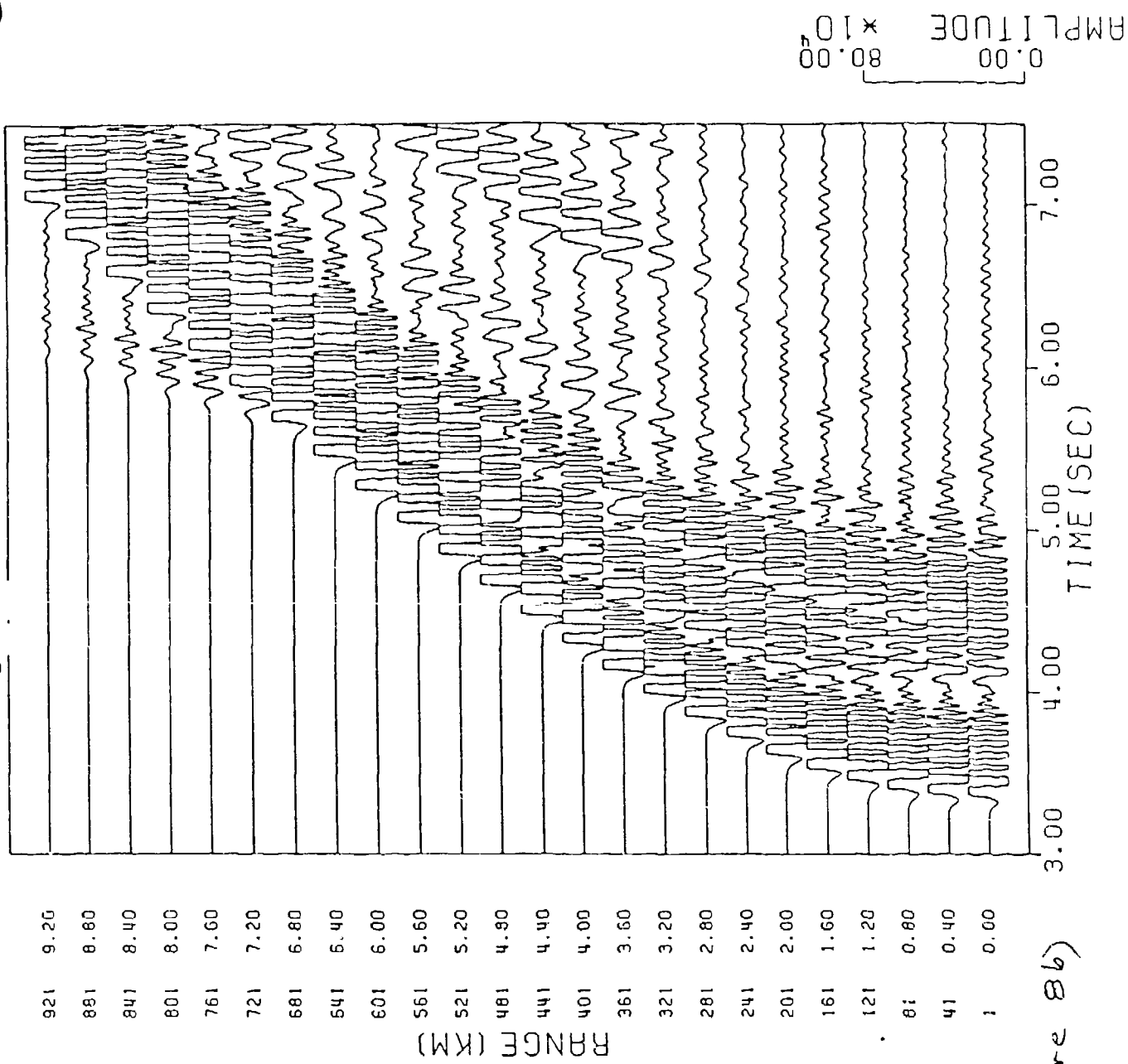can be seen at about 4.5 secs on the 0.0 and 0.4 km traces.

AMPLITUDE ×10⁴

0.00   80.00   0.00

RANGE (KM)

921	9.20
881	8.80
841	8.40
801	8.00
761	7.60
721	7.20
681	6.80
641	6.40
601	6.00
561	5.60
521	5.20
481	4.80
441	4.40
401	4.00
361	3.60
321	3.20
281	2.80
241	2.40
201	2.00
161	1.60
121	1.20
81	0.80
41	0.40
1	0.00

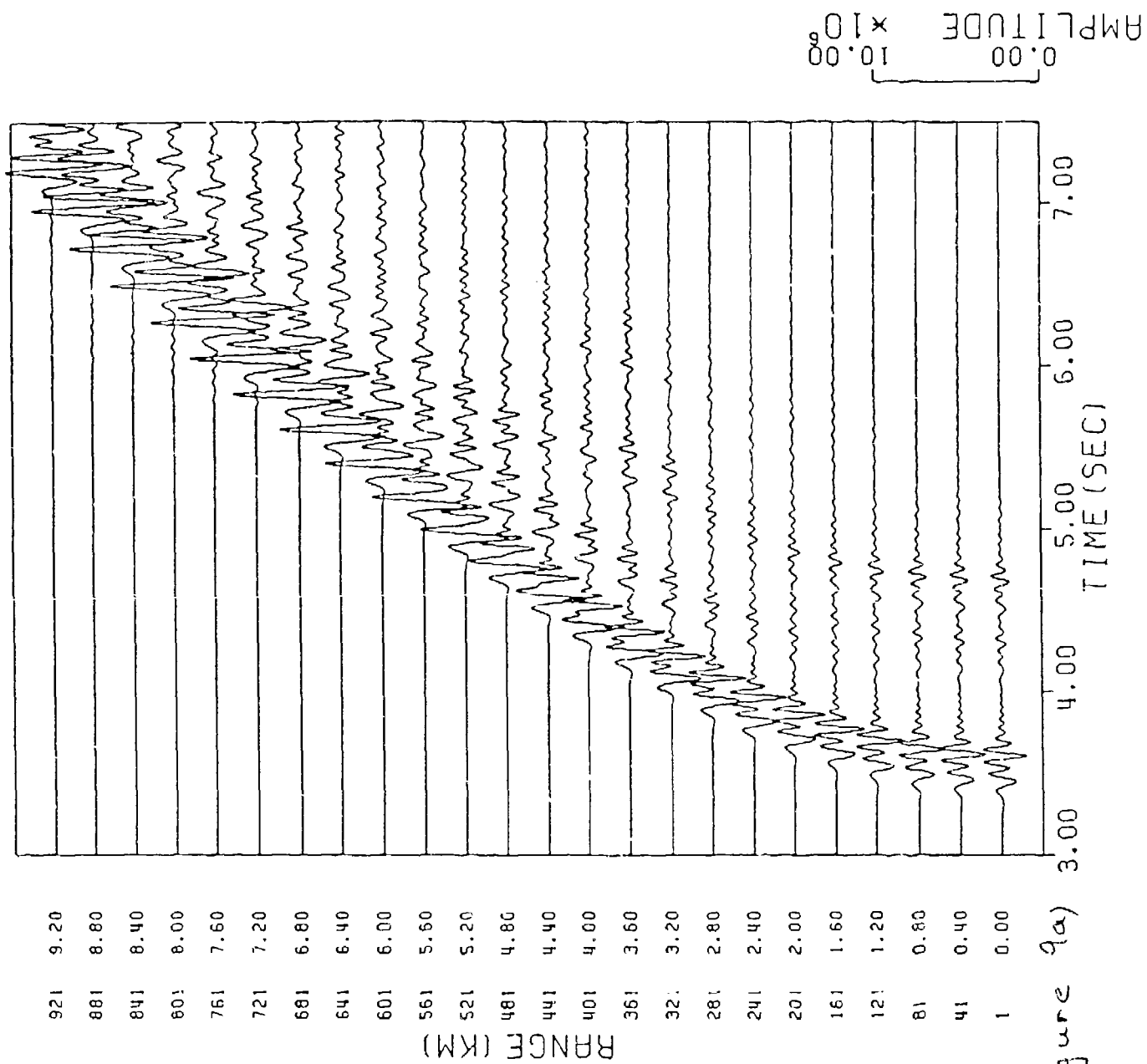TIME (SEC)

3.00   4.00   5.00   6.00   7.00

Figure 8b)

Figure 9. Time series results for a line of pressure receivers at 4.98 km depth in model BBNY6 (see Figure 2). This model is more rigid than BBNY1 and shows significantly different results at ranges greater than 2.0 km.

AMPLITUDE. ×10⁻⁴

0.00   80.00   0.00

RANGE (KM)

921	9.20
881	8.80
841	8.40
801	8.00
761	7.60
721	7.20
681	6.80
641	6.40
601	6.00
561	5.60
521	5.20
481	4.80
441	4.40
401	4.00
361	3.60
321	3.20
281	2.80
241	2.40
201	2.00
161	1.60
121	1.20
81	0.80
41	0.40
1	0.00

TIME (SEC)

3.00   4.00   5.00   6.00   7.00
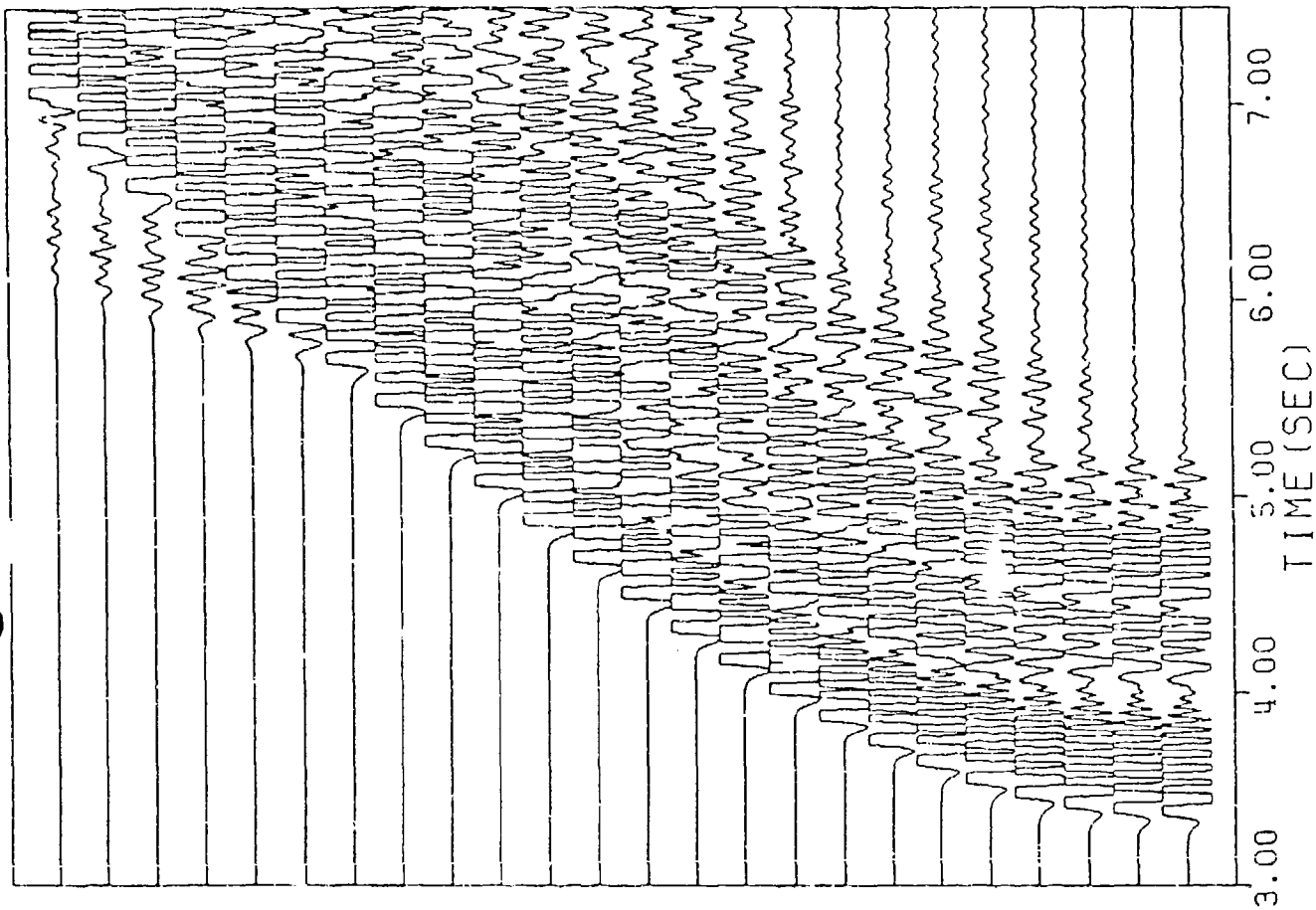
Figure 9b)

CONCLUSIONS

The results of the test models show that the finite difference code at NORDA is stable and producing reasonable results for large scale models including the whole water column. Further work should involve applications of the code to specific problems.

REFERENCES

Dougherty, M.E. and Stephen, R.A., 1987. Geoacoustic scattering from seafloor features in the ROSE area. J. acoust. Soc. Am., **82**, 238-256.

Dougherty, M.E. and Stephen, R.A., 1988. Seismic energy partitioning and scattering in laterally heterogeneous ocean crust. J. Pure and Applied Geophysics, **128**, 195-229.

Hunt, M.M., Gove, L.A., and Stephen, R.A., 1983. Findif: A software package to create synthetic seismograms by finite differences. WHOI Technical Memorandum, WHOI-83-42.

Stephen, R.A., 1983. A comparison of finite difference and reflectivity seismograms for laterally homogeneous marine models. Geophys. R.J. astr. Soc., **72**, 39-57.

Stephen, R.A., 1984. Finite difference seismograms for laterally varying marine models. Geophys. J.R. astr. Soc., **79**, 184-198.

Stephen, R.A., 1988. Lateral heterogeneity in the upper oceanic crust at DSDP Site 504. J. Geophys. Res., **93**, 6571-6584.

Stephen, R.A., 1988. A review of finite difference methods for seismo-acoustic problems at the sea floor. Reviews of Geophysics, **26**, 445-458.

Stephen, R.A., submitted. Solutions to range dependent benchmark problems by the finite difference method. J. acoust. Soc. Am.

Stephen, R.A., Pardo-Casas, F., and Cheng, C.H., 1985. Finite difference synthetic acoustic logs. Geophysics, **50**, 1588-1609.

Virieux, J., 1986. P-wave propagation in heterogeneous media: velocity-stress finite difference method, Geophysics, **51**, 889-901.